976 nm single-frequency distributed Bragg reflector fiber laser

Xiushan Zhu,[1,2,*] Wei Shi,[1] Jie Zong,[1] Dan Nguyen,[1] Robert A. Norwood,[2] Arturo Chavez-Pirson,[1] and N. Peyghambarian[1,2]

[1]*NP Photonics Inc., 9030 S. Rita Road, Tucson, Arizona 85747, USA*

[2]*College of Optical Sciences, University of Arizona, 1640 E. University Boulevard, Tucson, Arizona 85721, USA*

**Corresponding author: xzhu@npphotonics.com*

Received June 13, 2012; revised September 1, 2012; accepted September 4, 2012; posted September 5, 2012 (Doc. ID 170255); published October 2, 2012

A single-frequency distributed Bragg reflector (DBR) fiber laser at 976 nm was developed with a 2 cm long highly ytterbium-doped phosphate fiber and a pair of silica fiber Bragg gratings. More than 100 mW of linearly polarized output was achieved from the all-fiber DBR laser with a linewidth less than 3 kHz. The outstanding features of this single-frequency laser also include ultralow relative intensity noise and high wavelength stability. This fiber laser is an excellent seeder for high-power 976 nm narrow-linewidth laser amplifiers that can be used for efficient coherent blue-light generation through frequency doubling.

OCIS codes: 060.3510, 140.3615, 140.3510, 140.3570.

Stable wavelength, single polarization state, narrow-linewidth laser sources below 1 μm are highly demanded for nonlinear wavelength conversion to generate coherent blue light [1–3] or even deep ultraviolet coherent sources. Compared to semiconductor lasers, fiber lasers have advantages of narrow linewidth, excellent beam quality, high wavelength stability, ultralow relative intensity noise (RIN), and super power scalability. Single-frequency ytterbium (Yb^{3+})-doped fiber lasers below 1 μm, namely the three-level Yb^{3+} fiber lasers, are of high interest because of their high efficiency, high stability, and high reliability. Owing to the high solubility of rare-earth ions in phosphate glass, high concentration rare-earth doped phosphate fibers have been fabricated to develop high-gain fiber amplifiers [4–6] and single-frequency distributed Bragg reflector (DBR) fiber lasers longer than 1 μm [4,6–9]. In this Letter, we report the first demonstration of a stable 976 nm single-frequency DBR fiber laser using a short length highly Yb^{3+}-doped phosphate fiber.

The energy level diagram of Yb^{3+} ions is shown in the inset of Fig. 1. The ground-state absorption of the 915 nm pump corresponds to a transition from the lowest level of the $^2F_{7/2}$ manifold to the upper level of the $^2F_{5/2}$ manifold. The transition from the lowest level of the excited state $^2F_{5/2}$ manifold to the lowest level of the ground state $^2F_{7/2}$ manifold (i.e., zero-line transition) produces the laser emission at 976 nm. The emission and absorption cross-sections of 6 wt.% Yb^{3+}-doped phosphate glass, as shown in Fig. 1, were obtained by measuring the transmission and the fluorescence of the glass sample and analyzing the data with the McCumber equation. Compared to Yb^{3+}-doped silica glass [10], Yb^{3+}-doped phosphate glass has a larger difference between the absorption and the emission cross-sections at short wavelengths [from zero-line wavelength (where $\sigma_{abs} = \sigma_{em}$) to 1 μm]. It makes Yb^{3+}-doped phosphate fiber a potential high-gain medium for fiber lasers below 1 μm. The lifetime of the Yb^{3+} ions was measured to be about 1.8 ms. The ready availability of fiber Bragg gratings (FBGs) at 976 nm and the desirability of 488 nm as an argon-ion replacement wavelength led us to pursue a 976 nm single-frequency fiber laser. However, because the absorption and emission cross-sections are comparable at 976 nm, intense pumping is required to excite 50% of the Yb^{3+}-ion population and create gain in the three-level laser system. On the other hand, due to the small excited population required for quasi-four-level transitions, spurious lasing or amplified spontaneous emission (ASE) at long wavelengths is prevalent. Spurious lasing and strong ASE are deleterious to single-frequency fiber lasers and amplifiers below 1 μm. Different approaches, including spectral gain discrimination [11], ring doping [12], air-clad fiber [3,13], solid-core photonic bandgap fibers [14], and a distributed feedback laser configuration [15] have been employed to effectively suppress spurious lasing and achieve high-power 980 nm fiber lasers and amplifiers. Here, we report that a core-pumped DBR fiber laser using a short length of highly Yb^{3+}-doped phosphate fiber can produce a 976 nm single-frequency laser with over 50 dB signal-to-noise ratio (SNR) and other attractive features.

The experimental configuration is depicted in Fig. 2. The single-frequency fiber laser chain was fabricated

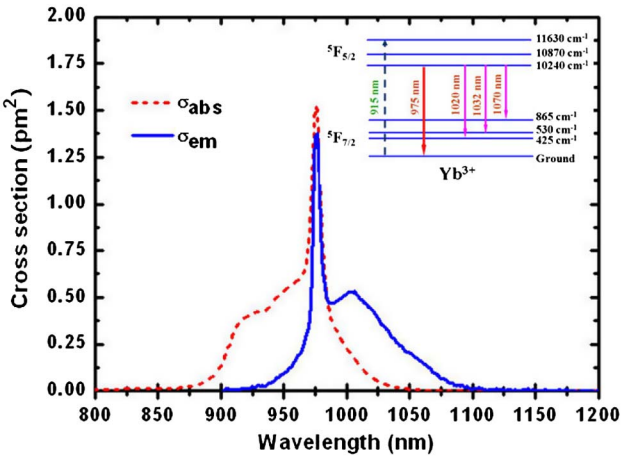

Fig. 1. (Color online) Absorption (red dashed curve) and emission (blue solid curve) cross-sections of Yb^{3+}-doped phosphate glass. (Inset: the energy level diagram of Yb^{3+} ions.)

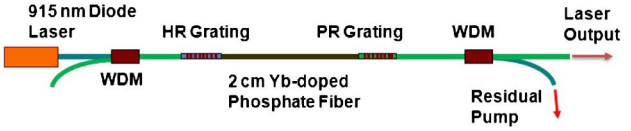

Fig. 2. (Color online) Depiction of a 976 nm Yb^{3+}-doped phosphate all-fiber DBR laser.

by cleaving high-reflection (HR > 99%) and partial-reflection (PR = 60%) FBGs very close to the index modulation region and directly splicing to a 2 cm-long highly Yb^{3+}-doped phosphate fiber fabricated and developed by NP Photonics. A robust and reliable fusion splice was achieved between phosphate gain fiber and silica fibers. Single frequency operation is ensured by a large free spectral range (FSR) determined by the short length of the laser cavity and the narrow bandwidth [full width at half-maximum <0.05 nm] of the PR FBG. Because the PR FBG was fabricated on a polarization maintaining (PM) optical fiber and the wavelength separation between the two PR peaks, corresponding to two linear polarization states, is larger than the 0.2 nm bandwidth of the HR FBG, single polarization operation can be achieved simultaneously. A fiber-coupled 915 nm diode laser pump was spliced to the pump port of a 915 nm/980 nm wavelength division multiplexer (WDM). The common port was then spliced to the HR FBG end of the fiber chain directly. The backward ASE can be delivered to the signal port of the WDM, while at the other end of the fiber chain, a PM WDM was spliced to the PR FBG to split the laser and the residual pump. The entire fiber laser was packaged in a NP standard Rock module, in which the laser stability and other features can be monitored and actively controlled. The highly stable fiber chain holding structure is important in achieving and maintaining low-noise single-frequency operation. The output power of the 976 nm single-frequency fiber laser as a function of the 915 nm pump power was measured as shown in Fig. 3. More than 100 mW output can be obtained when the launched pump power is about 450 mW. The efficiency of the 976 nm single-frequency fiber laser is about 25% (the output power versus the launched pump power), which is smaller than that (40%) of a

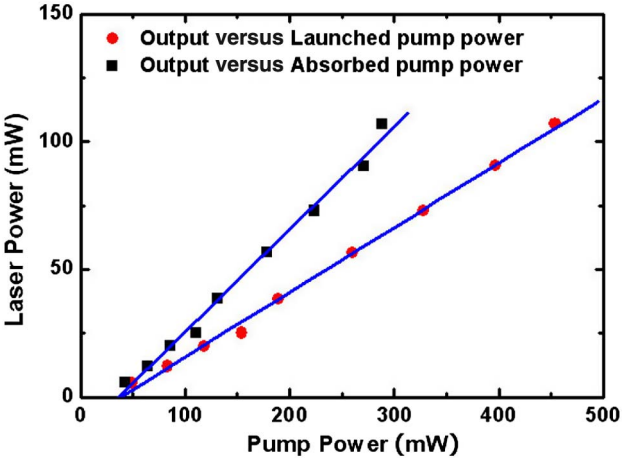

Fig. 3. (Color online) Output power of the 976 nm single-frequency fiber laser as a function of the launched pump power.

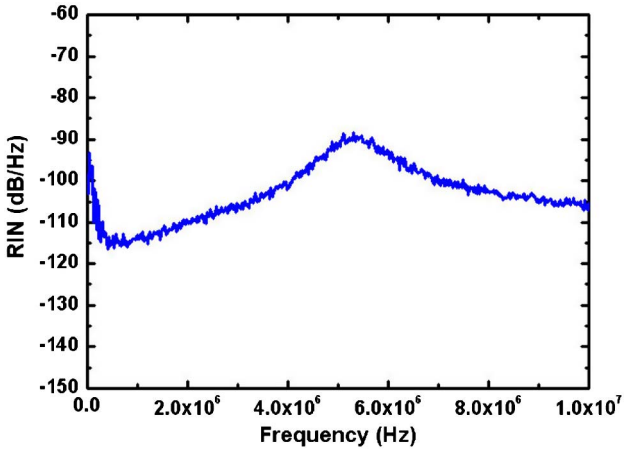

Fig. 4. (Color online) Relative intensity noise of the 976 nm single-frequency DBR fiber laser.

975 nm Yb^{3+}-doped phosphate fiber laser reported by Bufetov *et al.* [16] because this all-fiber laser involves the insertion loss of the two WDMs (0.7 dB/each) and the splicing loss of many splice joints (0.1–0.2 dB/joint). Since a large amount of pump is residual, the efficient can be 40% if the residual pump is excluded as shown in Fig. 3. Therefore, the efficiency can be improved by optimizing the gain fiber length and the doping level [17] and reducing the losses in the cavity. The RIN was measured as shown in Fig. 4 when the output power is 68 mW. The RIN is below −110 dB/Hz around 1 MHz, so the intensity stability of this single-frequency fiber laser can be estimated to be better than 0.001%. The peak at 5.4 MHz corresponds to the relaxation oscillation of Yb^{3+} ions. The spectrum of the laser operating at 100 mW was measured by an optical spectrum analyzer (OSA) and is shown in Fig. 5. Clearly, this single-frequency fiber laser has an SNR of more than 50 dB and there is no strong ASE or spurious lasing at long wavelengths even at the maximum pump power. The inset shows the spectrum of the laser measured with an OSA (AnDo, AQ6317B) with a resolution of 0.01 nm. The polarization extinction ration (PER) of this fiber laser was measured by using a linear polarizer and a power

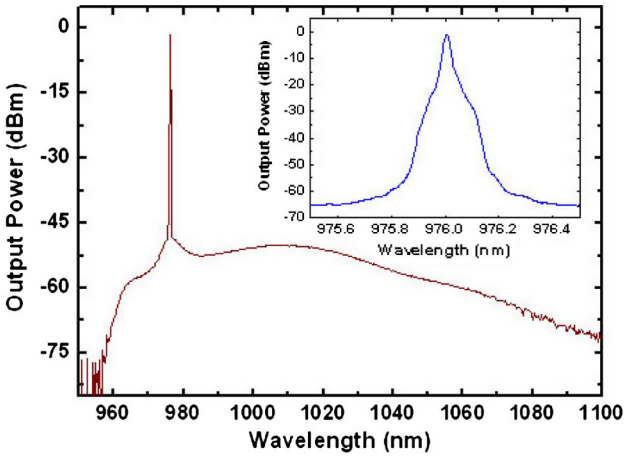

Fig. 5. (Color online) Output spectrum of the 976 nm single-frequency DBR fiber laser. (Inset: laser spectrum measured by an OSA with 0.01 nm resolution.)

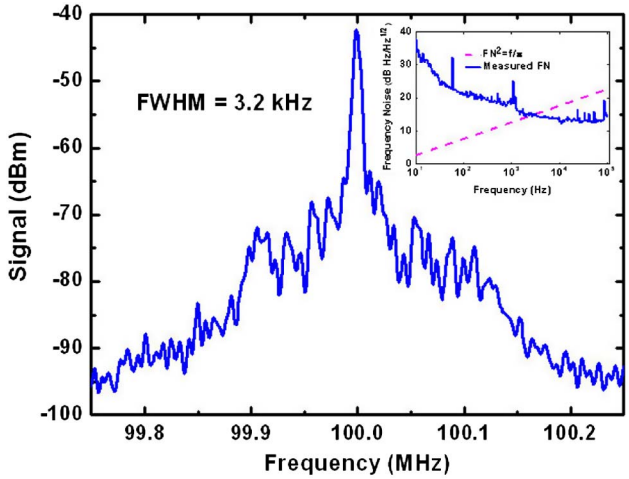

Fig. 6. (Color online) The measurement result of the delayed self-heterodyne interferometer for the 976 nm single-frequency DBR fiber laser. Inset: The measured FN and a magenta line plotted with equation $FN^2 = f/\pi$.

meter. More than 20 dB of PER sufficiently confirms the single-frequency and single-polarization operation of this fiber laser. In order to facilitate cavity enhanced frequency doubling and also to achieve stable second-harmonic generation (SHG), the wavelength of the single-frequency fiber laser was stabilized by keeping the fiber laser cavity temperature fixed. The wavelength stability was measured by monitoring the center wavelength of the fiber laser for 2.5 h. The variation of the center wavelength is less than 0.0005 nm during the measurement period. This corresponds to the free-running wavelength stability. Further improvements are possible by active feedback to the laser cavity. The linewidth of the single-frequency fiber laser was measured using the method of delayed self-heterodyne interferometery. The delay line was 100 km and the resolution was about 2 kHz. The measurement result is shown in Fig. 6, where the 3 dB bandwidth of 3.2 kHz indicates a fiber laser linewidth of about 1.6 kHz. Since the linewidth enhancement of DBR fiber lasers mainly originates from thermal noise, acoustic noise, and pump fluctuations more than spontaneous emission like semiconductor lasers [18], the method of delayed self-heterodyne may be not able to determine the linewidth of fiber laser accurately [19]. Frequency noise (FN) was also measured (shown by the blue curve in the inset of Fig. 6) and used to estimate the linewidth by evaluating πFN^2 [18,20]. According to the measurement results of delayed self-heterodyne and frequency noise, the linewith of the 976 nm single-frequency fiber laser was estimated to be less than 3 kHz.

In conclusion, a 976 nm single-frequency DBR fiber laser was developed based on highly Yb^{3+}-doped phosphate fiber, for the first time. This all-fiber single-frequency laser with attractive features can be used for efficient blue and UV generation through nonlinear frequency conversion. Moreover, this high-performance 976 nm single-frequency fiber laser can be used as a single-frequency, low RIN pump laser for long wavelength Yb^{3+}-, Er^{3+}-, or Yb^{3+}/Er^{3+}-doped fiber lasers and amplifiers.

This work was supported by the Army STTR Project "Deep UV Laser Source for Raman Spectroscopy" under contract no. W31P4Q-11-C-0276.

References

1. D. B. S. Soh, C. Codemard, S. Wang, J. Nilsson, J. K. Sahu, F. Laurell, V. Philippov, Y. Jeong, C. Alegria, and S. Baek, IEEE Photon. Technol. Lett. **16**, 1032 (2004).
2. S. Zou, P. Li, L. Wang, M. Chen, and G. Li, Appl. Phys. B **95**, 685 (2009).
3. V. Prosentsov, E. Sherman, A. Patlahn, Y. Ariel, and D. Eger, Proc. SPIE **4974**, 193 (2003).
4. A. Chavez-Pirson, Proc. SPIE **7839**, 78390K (2010).
5. W. Shi, E. B. Peterson, Z. Yao, D. T. Nguyen, J. Zong, M. A. Stephen, A. Chavez-Pirson, and N. Peyghambarian, Opt. Lett. **35**, 2418 (2010).
6. Y. Lee, M. J. F. Digonnet, S. Sinha, K. E. Urbanek, R. L. Byer, and S. Jiang, IEEE J. Sel. Top. Quantum Electron. **15**, 93 (2009).
7. M. Leigh, W. Shi, J. Zong, J. Wang, S. Jiang, and N. Peyghambaian, Opt. Lett. **32**, 897 (2007).
8. J. Geng, C. Spiegelberg, and S. Jiang, IEEE Photon. Technol. Lett. **17**, 1827 (2005).
9. Y. Kaneda, Y. Hu, C. Spiegelberg, J. Geng, and S. Jiang, in *OSA Topical Meeting on Advanced Solid-State Photonics* (2004), paper PD5.
10. R. Paschotta, J. Nilsson, A. C. Tropper, and D. C. Hanna, IEEE J. Quantum Electron. **33**, 1049 (1997).
11. L. A. Zenteno, J. D. Minelly, A. Liu, A. J. G. Ellison, S. G. Crigler, D. T. Walton, D. V. Kuksenkov, and M. J. Dejneka, Electron. Lett. **37**, 819 (2001).
12. J. Nilsson, J. D. Minelly, R. Paschotta, A. C. Tropper, and D. C. Hanna, Opt. Lett. **23**, 355 (1998).
13. R. Selvas, J. K. Sahu, L. B. Fu, J. N. Jang, J. Nilsson, A. B. Grudinin, K. H. Yia-Jarkko, S. A. Alam, P. W. Turner, and J. Moore, Opt. Lett. **28**, 1093 (2003).
14. L. B. Fu, M. Ibsen, D. J. Richardson, and D. N. Payne, IEEE Photon. Technol. Lett. **16**, 2442 (2004).
15. V. Pureur, L. Bigot, G. Bouwmans, Y. Quiquempois, M. Douay, and Y. Jaouen, Appl. Phys. Lett. **92**, 061113 (2008).
16. I. A. Bufetov, S. L. Semenov, A. F. Kosolapov, M. A. Mel'kumov, V. V. Dudin, B. I. Galagan, B. I. Denker, V. V. Osiko, S. E. Sverchkov, and E. M. Dianov, Quantum Electron. **36**, 189 (2006).
17. J. R. Armitage, R. Wyatt, B. J. Ainsly, and S. P. Craig-Ryan, Electron. Lett. **25**, 298 (1989).
18. E. Ronnekleiv, Opt. Fiber Technol. **7**, 206 (2001).
19. P. Horak and W. H. Loh, Opt. Express **14**, 3923 (2006).
20. G. D. Domenio, S. Schilt, and P. Thomann, Appl. Opt. **49**, 4801 (2010).